Environmental and Climate Technologies
2022, vol. 26, no. 1, pp. 199–212
https://doi.org/10.2478/rtuect-2022-0016
https://content.sciendo.com

A New Method for the Rapid Synthesis of Gas Hydrates for their Storage and Transportation

Anatoliy M. PAVLENKO[1*], Hanna KOSHLAK[2]

[1,2]*Department of Building Physics and Renewable Energy, Kielce University of Technology, Kielce, Poland*

***Abstract* – This presents the analysis of the main reasons for a significant decrease in the intensity of diffusion processes during formation of gas hydrates; solutions to this problem are proposed in a new process flow diagram for the continuous synthesis of gas hydrates. The physical processes, occurring at corresponding stages of the process flow are described in detail. In the proposed device, gas hydrate is formed at the boundary of gas bubbles immersed in cooled water. The dynamic effects arising at the bubble boundary contribute to destruction of a forming gas hydrate structure, making it possible to renew the contact surface and ensure efficient heat removal from the reaction zone. The article proposes an assessment technique for the main process parameters of the synthesis of gas hydrates based on the criterion of thermodynamic parameters optimization.**

***Keywords* – Continuous cycle of hydrate formation; gas hydrates; intensity of heat; mass transfer processes at the interface**

1. INTRODUCTION

The industrial use of gas hydrates (GM) can be used as a very important source of energy for all people. In many countries, gas hydrates are considered as the most likely alternative fuel [1]–[3]. Global estimates of the gas content in hydrate structures are within the range of ≈(1–5) 10^{15} m^3 [4]–[8]. The works of many authors [9]–[11] provide information on the presence of GH natural sources in various geological structures. However, lack of sufficient information on the features of their formation and decomposition hinders active implementation of gas hydrate technologies. At present, significant efforts of many researchers are aimed at solving these problems to improve future efficiency of GM production, synthesis, storage, transportation and industrial use. We are going to analyse gas hydrate synthesis technology that will guarantee its transportation and long-term storage. According to many researchers [12]–[15], storage of natural gas in clathrate hydrates offers the safest, cleanest and most compact storage method, explained by the relative convenience of natural gas recovery at minimal cost compared to conventional storage methods [16]–[21]. Works [22] and [23] present comprehensive data on the production, storage and transportation of gas hydrates and proves practicality of transportation and storage of gases in a hydrated state.

GM synthesis is one of the main stages of such technology. Clearly, this process shall be fast, continuous, relatively simple and inexpensive. The stochastic character of hydrate nucleation and slow kinetics of hydrate growth are the main problems to be addressed during GM synthesis; they are analysed in the works of above-mentioned researchers. Deterministic and rapid nucleation combined with fast crystallization kinetics would allow the use of this

* Corresponding author.
E-mail address: apavlenko@tu.kielce.pl

©2022 Author(s). This is an open access article licensed under the Creative Commons Attribution License (http://creativecommons.org/licenses/by/4.0).

technology for commercial applications. These are the first two problems we are going to focus on. The nucleation process could be determined to some extent if ready-made hydrate formation centres were introduced into the reaction zone. We will demonstrate this process as it was performed in our GM synthesis technology. As for the second problem, the hydrate formation rate, in our opinion, it is the hydrate itself that causes a significant decrease in the intensity of diffusion flows in the reaction zone. Diffusion processes have also been studied by many authors [24]–[27], however, in their works, the transfer process itself was considered with no consequent conclusions regarding sufficiently high intensity of mass transfer. Currently, in the literature references, you can have a description of many devices for GM production [28]–[35], where the main attention was paid to methods used to increase the gas and liquid contact area: either by dispersing water in a gas or formation of a bubble gas flow in water. For this purpose, it is possible to use, for example, bubble columns, bubblers or spray reactors [36]–[41]. In [42], during study of GM synthesis in a bubble column, the authors observed a thin hydrate film formation on the gas bubble surface, where GM is gradually formed. However, the rate of gas hydrate formation was not high, and the process itself cannot be continuous, due to the fact that gas bubbles with a hydrate crust agglomerated into large complexes, where the synthesis practically stopped. Gas mixing, spraying and bubbling are known methods of GM synthesis intensification [43]–[45]. Mixing helps to mix the gas and liquid phases and increase the phase interface surface, increasing GM synthesis rate. To increase the synthesis process intensity, various chemical activating agents were also used and described in these works. Efficient heat removal from the reaction zone is the third problem to be solved. The heat removal rate significantly affects GM synthesis rate. In every cited study the hydrate synthesis rate decreases over time due to changes in thermodynamic parameters in the hydrate formation reaction zone. In our study, we consider the mechanical activation of GM synthesis, following a different concept – the intensity of GM synthesis process is determined not only by the liquid volume or the size of the phase contact area, but mainly by the intensity of phase interface renewal, which in turn increases the intensity of heat removal from the reaction zone. Therefore, GM synthesis technologies should also be evaluated in terms of the phase interface renewal rate. Hydrate films, formed on the bubbles surface, create resistance to heat removal during the exothermic hydrate formation reaction. On the other hand, these films at a certain stage of their formation can be easily destroyed by appropriate hydrodynamic and thermodynamic instability in the reactor, contributing to a constant intensive phase interface renewal and increase of hydrate formation rate. Thus, the drop, bubble, or combined modes of gas hydrate formation and relevant devices can be sufficiently effective for fast hydrate formation. However, the problems of deterministic hydrate nucleation, low intensity of hydrate formation, hindered by hydrate formation at the interface, ineffective heat removal from the reaction zone of hydrate formation and removal of excess water from the finished hydrate, are still to be addressed.

2. Process Flow the Diagram of GM Synthesis

This study is represented by the development of the ideas, specified in [46]. Based on the analysis of GM synthesis devices, cited in Section 1, we have developed an injection reactor (Fig. 1) to solve the problems of hydrate crust breaking at the interface, intensive heat removal from the reaction zone formation of the developed phase contact area.

The hydrate crust breaking contributes to renewal of the phase contact surface, intensity of mass transfer processes remains quite high. The broken crusts are continuously removed from reactor 1 to separator 2, water after hydrate separation returns to the reactor. Hydrate crystals enter the reactor with the recirculation water, they become the centres of hydrate structure

formation. This technology requires a separator, but it makes it possible to solve these problems and organize a continuous synthesis process.

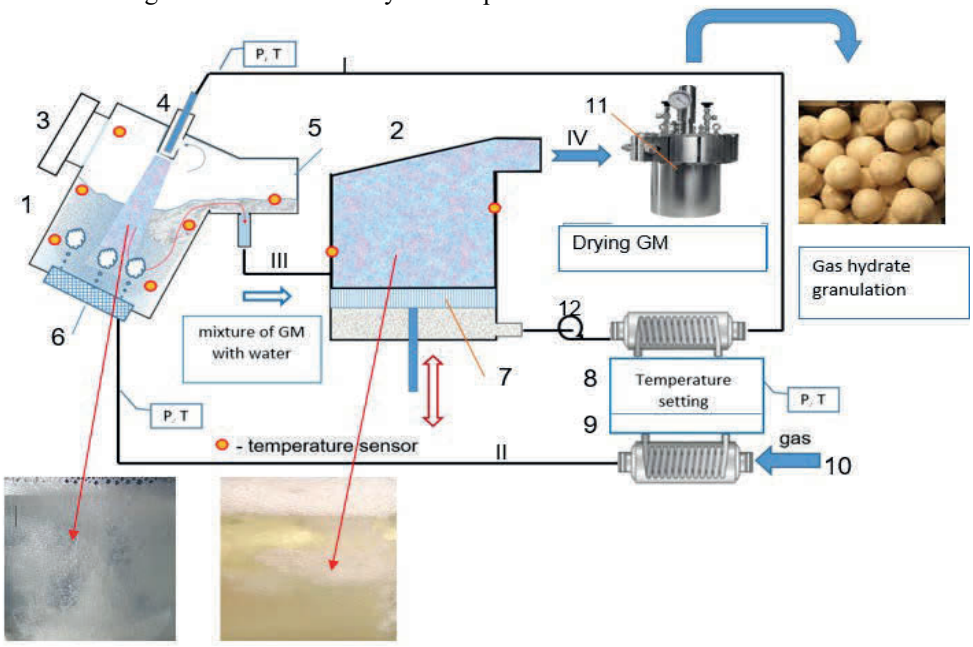


Fig. 1. Scheme of a gas hydrate plant for continuous production of gas hydrate: 1– reactor; 2 – separator 2 – temperature sensors; 3, 5 – inspection windows; 4 – jet apparatus; 5 – removal of water-gas hydrate mixture; 6 – bubbler; 7 – filter; 8, 9 – thermostats; 10 – gas; 11 – thermal chamber for hydrate drying; 12 – recirculation pump; flows: I – water under pressure; II – gas; III – water-gas hydrate mixture; IV – wet hydrate for drying.

Fig. 2 shows the scheme of gas-liquid mixture formation. In injection nozzle 4 (Fig. 1) part of the gas from the reactor zone enters the water jet and mixes. When the jet enters liquid volume, gas is injected into the liquid and dispersed with formation of the smallest bubbles. Gas pressure in the bubbles changes cyclically, deforming the surface of bubbles.

The amount of injected gas depends on the nozzle geometric parameters and hydrodynamic mode of liquid flow.

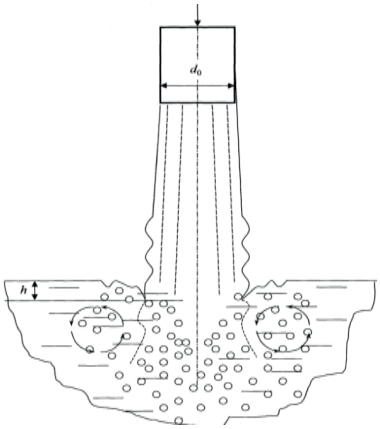


Fig. 2. Scheme of gas-liquid mixture formation.

Gas bubbles, in the process of hydrate crust formation around them, will be subjected to variable deformation, resulting from pressure change in the middle of bubbles and mechanical action of the liquid jet. At the same time there will be constant crust breaking as gas bubbles change their size and form.

The proposed GM production procedure in a continuous process will occur at constant parameters. The reactor pressure is maintained automatically by compensating for the appropriate amount of gas that has entered the gas hydrate. For continuous GM synthesis, it is necessary to provide conditions for its constant removal from the reactor, supply of gas and water to the reactor, as well as heat removal during hydrate formation. Hydrate removal from the reactor is complicated by a rapid agglomeration of hydrate structures (broken GM crusts).

To prevent this process, the GM concentration in the mixture shall not exceed 15–17 %.

Water, separated from water-gas-hydrate mixture in the separator, returns to the reactor, containing many microstructures and hydrate formation 0.1–0.5 mm nuclei. The hydrate formation rate at this phase contact is quite high, depending on the reaction zone temperature, which in turn depends on the heat removal rate of GM synthesis reaction.

3. MAIN PROCESS STEPS

3.1. Water Removal from Gas Hydrate Mass

In Separator 2 (Fig. 1) most of the water is separated from the hydrate mixture. However, it is problematic to remove adsorbed water by separation. In our previous experiments on the presented installation, the separation coefficient was up to 0.83–0.85. To produce a dry gas hydrate, the cooled gas hydrate mixture, obtained in the separator, contacts with gas under certain thermodynamic conditions in thermal chamber 11 (Fig. 1). In this case, a considerable total surface pore area provides a sufficient contact phases area for intensive hydrate formation.

The following gas was used for the experiment: CH_4 – 92.8 %, C_2H_6 – 5.1 %, C_3H_8 – 2.1 %. The nozzle diameter was 2.12 mm. Gas pressure in the reactor was maintained at 3.8 MPa. The temperature in a plant thermal chamber was maintained at 276.1 K. The distance from the nozzle 4 (Fig. 1) of the jet apparatus to the liquid surface was 98 mm. Water was supplied into the nozzle under 10 MPa with $1.3 \cdot 10^{-3}$ m^3/s flow rate. As a result of pressure drop between pump 12, separator 2 and reactor 1, water-gas hydrate mixture circulated from the reactor to the separator. Wet gas hydrate mixture was subjected to the final stage of processing in contact apparatus 11, where GM final properties were formed. Hydrate formation heat is removed in thermostat 9. The rate of gas hydrate formation was determined by the amount of gas consumed per unit time.

3.2. Hydrate Mass Drying

The hydrate mass is dried by its contact with hydrate-forming gas (in this case, a gas of similar composition) in thermal chamber 11 (Fig. 1). When a hydrate mass layer is treated with gas under pressure, free water binds to the hydrate.

The crushed hydrate mass (with particle size not more than 1 mm) was placed in a cylindrical container, 0.65 m long and 0.1 m in diameter. Gas was supplied to the container, pressure and temperature were recorded. The gas pressure in a container was raised to 5 MPa at 273.5 K. This temperature was maintained throughout the drying process.

The hydrate structure and its properties change during processing (Fig. 3). Hydrate in Fig. 3(b) is ready for formation into blocks or granules (Fig. 4).



(a) (b) (c)

Fig. 3. GM photos: a) 15 % water content, morphology 1 (M1); b) 6 % humidity, morphology 2 (M2); c) dry hydrate, morphology 3 (M3).



Fig. 4. Formed hydrate (morphology 2 (M2)).

Fig. 5 shows a thermogram of hydrate formation process in a dehumidifier. Layer temperature sensors recorded the temperature change over time. Pressure in the dehumidifier was rising stepwise. The change in pressure was accompanied by a change in the hydrate structure. during drying.

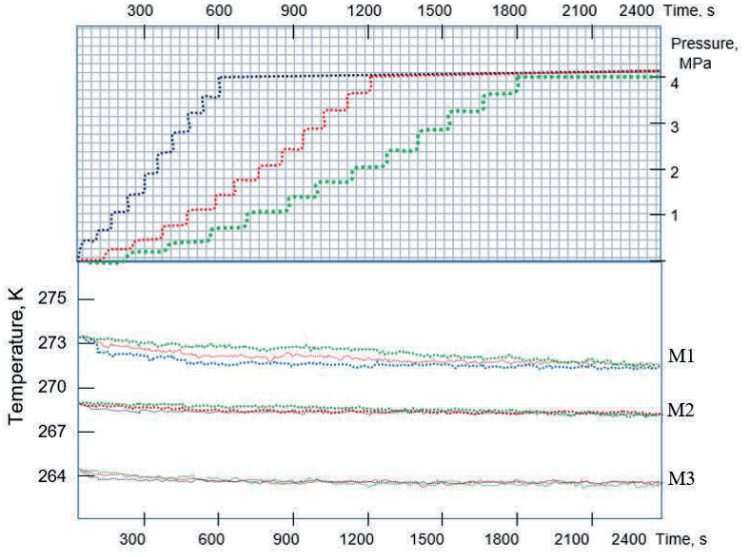


Fig. 5. Thermograms of hydrate formation at the final stage.

As shown in Fig. 5, the pressure injection process was completed in about 10 minutes. The whole formation process lasts 40 minutes. Prior to processing, morphology of the hydrate containing the experimental medium is a significant inhomogeneity (Fig. 3(a)). Adsorbed water formed GM.

Fig. 5 shows the temperature trajectories during the hydrate formation process. Temperatures in various experiments ranged from 273.5 to 265 K. The decrease in temperature indicated a more intense process. However, decrease in temperature below the minimum specified value resulted in GM drying with final morphology (Fig. 3(c)), not suitable for pressing the hydrate into granules with a stable structure.

3.3. General Process Flow Diagram of GH Synthesis

Fig. 6 shows a GM synthesis diagram, including the main processes: hydrate mass formation, separation, adsorbed water binding and formation of gas hydrate granules or blocks suitable for transportation and storage. If GM is used for heat accumulators, then the final stage of hydrate formation shall be implemented at low temperature (Fig. 5, Fig. 3(c)).

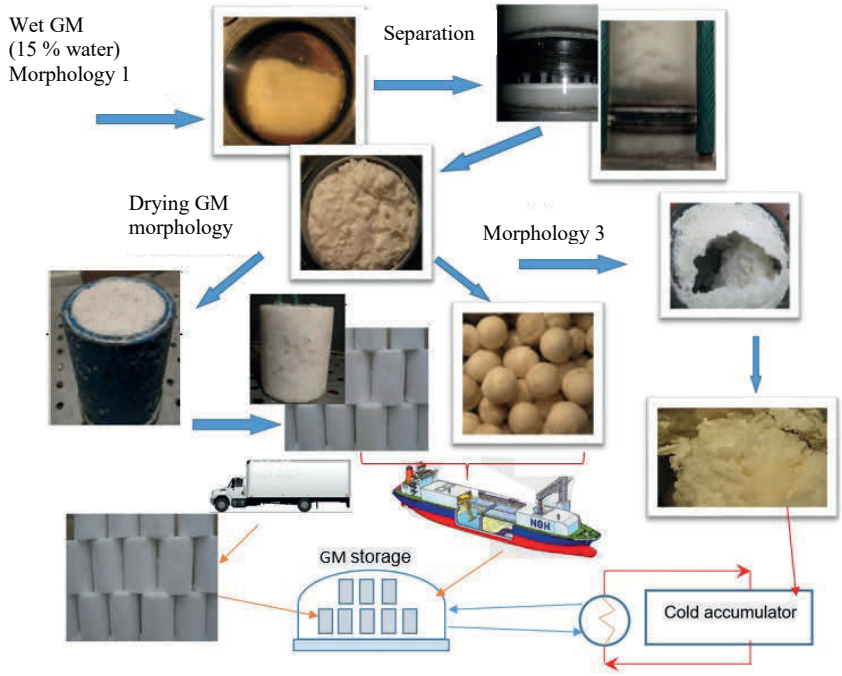


Fig. 6. GM synthesis diagram.

Optimal thermobaric conditions of the hydrate formation process in reactor 1 were determined experimentally and are presented in Fig. 7 by the equilibrium hydrate formation curve.

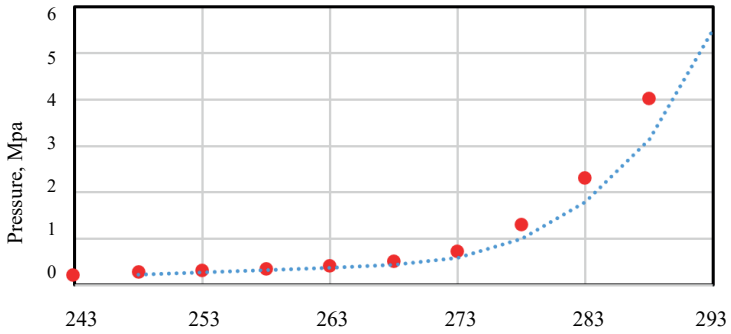


Fig. 7. Equilibrium curve of hydrate formation for the gas, entering the reactor.

After empirical data processing, the equation, describing the process of gas hydrate formation in the reactor is as follows:

$$R = 0.117 \cdot V(k_m - 3.15)1.15(c_{sol} - c_b), \tag{1}$$

where

c_{sol} Gas concentration at the gas-liquid interface at hydrate formation pressure and equilibrium temperature, mol/m^3;

c_b Gas concentration in the liquid at hydrate formation pressure and equilibrium temperature, mol/m^3;

v_0 Volumetric flow rate, m^3/s; mass transfer coefficient k_m depends on nozzle diameter d_0, liquid volume in reactor V and is determined by the formula

$$k_m = \frac{5.4 \cdot 10^{-6} (\rho \cdot d_0^3 \cdot v_0^3)}{\sigma \cdot V} \left[\frac{l}{d_0} \right], \tag{2}$$

where

ρ Water density, kg/m^3;

σ Surface tension of liquid, $4.56 \cdot 10^{-2} - 7.33 \cdot 10^{-2}$, N/m;

l Injector nozzle length.

4. Heat Exchange Processes on the Interfacial Surface

The hydrate formation is based on heat and mass transfer processes. Each process under certain conditions can limit the reaction rate. But with the optimal ratio of heat and mass transfer processes, GM can be produced rather quickly.

Our experimental data [46] are generalized by empirical equation

$$\frac{\beta_v l^2}{D_r} = 0.042 \cdot \mathrm{Re} \cdot Sc^{0.45} = 0.042 \frac{v_g l}{v_r} \left(\frac{v_r}{D_r} \right)^{0.45}, \tag{3}$$

where

β_V Volume mass transfer coefficient from gas to liquid, s^{-1}; $\beta_V = \beta_F \cdot S_V$;

Sc Schmidt number;

l Capillary constant;

D_r Coefficient of molecular diffusion of gas into liquid;

v_r Liquid volume;
v_g Gas volume.

Capillary constant:

$$l = \sqrt{\frac{\sigma}{\rho_\gamma g}} . \tag{4}$$

Surface coefficient of mass transfer from gas to liquid with energy dissipation rate E in liquid:

$$\beta_F = 0.24\sqrt{D_r\left(\frac{E}{V_r}\right)^{0.5}} . \tag{5}$$

According to the law of convective diffusion, the amount of gas transmitted to water surface,

$$M = \beta_F \cdot \Delta C \cdot F \cdot \tau . \tag{6}$$

To optimize GM synthesis, it is necessary to correlate heat and mass transfer processes on the phase interfacial surface. We propose to apply the optimization criterion, which can be obtained by considering the system of equations of heat and mass transfer at the phase interfacial surface, W/m^2 and kg/(s·m^2)

$$\begin{cases} q = \alpha(T_\Gamma - T_0) \\ \Delta M = \beta_F(\rho_0 - \rho_\Gamma), \\ q = \dfrac{\Delta M_r}{\overline{m}_g} \end{cases} \tag{7}$$

where $\overline{m}_g$ is mass gas content of gas hydrate, kg/kg.

Substitution from the system of equations (7) gives the ratio, °C·m^3/kg

$$\frac{(T_\Gamma - T_0)}{(\rho_0 - \rho_\Gamma)} = \frac{\beta_F r}{\alpha \overline{m}_g} . \tag{8}$$

Using Nusselt's criteria for heat transfer $Nu = \dfrac{\alpha l}{\lambda}$ and diffusion $Nu' = \dfrac{\beta_F l}{D}$, the right-hand side of Eq. (8) can be rewritten as

$$\frac{\beta_F r}{\alpha \overline{m}_g} = \frac{Nu'}{Nu}\frac{Dr}{\lambda \overline{m}_g}, \tag{9}$$

where the ratio of Nusselt's criteria is a criterion for GH synthesis optimization.

$$K_s = \frac{Nu'}{Nu} \tag{10}$$

To determine K_S value, express the gas density through pressure and temperature from the thermodynamic state equation

$$\rho = \frac{P\mu}{RTZ} \tag{11}$$

In mass-transfer apparatus the processes occur under constant pressure conditions, compressibility coefficient Z changes little. In this case, the difference in densities from Eq. (8) can be determined by the temperature difference, kg/m^3

$$\rho_0 - \rho_\Gamma = \frac{P\mu}{RT_0Z} - \frac{P\mu}{RT_\Gamma Z} = \frac{P\mu}{RZ}\left(\frac{1}{T_0} - \frac{1}{T_\Gamma}\right). \tag{12}$$

Given the difference in gas densities, Eq. (8) takes the form

$$\frac{(T_\Gamma - T_0)}{\left(\frac{1}{T_0} - \frac{1}{T_\Gamma}\right)} = K_S \frac{DP\mu r}{\lambda RZ\overline{m_g}}. \tag{13}$$

It may be demonstrated that

$$\frac{(T_\Gamma - T_0)}{\left(\frac{1}{T_0} - \frac{1}{T_\Gamma}\right)} = T_0 \cdot T_\Gamma. \tag{14}$$

Considering Eq. (14) from Eq. (13), we obtain the optimization criterion value

$$K_S = \frac{D_g P\mu_g r_{gg}}{\lambda_g R_\mu Z\overline{m_{gg}} T_r T_g}, \tag{15}$$

where

$\overline{m}_{gg}$ Mass content of gas in GM, kg/kg;
T_r Liquid temperature, K;
T_g Gas temperature, K;
P Pressure, at which the synthesis process occurs, Pa;
r_{gg} Heat of GM dissociation, J/kg.

Non-dimensional optimization coefficient of GM synthesis determines the optimal ratio between heat and mass transfer processes near the interfacial surface under hydrate formation depending on the thermophysical characteristics of gas hydrate and its synthesis conditions, or in other words, the coefficient determines the optimal ratio of diffusion processes and mass transfer at the phase interface.

For conditions of GM synthesis for different gases, we propose the optimal values of K_S, presented in Table 1.

TABLE 1. THE OPTIMIZATION COEFFICIENT VALUE FOR DIFFERENT GASES

Gas	K_S
Methane	36–40
Ethane	55–57
Propane	115–124
Isobutane	173–186

The physical content of the coefficient can be interpreted as follows – to maintain the maximum rate of GM formation, the intensity of heat transfer processes (heat removal from the reaction zone) near interfacial surface shall exceed the intensity of mass transfer processes by 36–40 times (e.g. for methane). In case of lower actual K_S values, the process of gas hydrate synthesis will be restricted to low intensity of heat removal, if the optimal value is exceeded – to low intensity of mass transfer processes.

Comparison of the actual value (K'_S) with the optimal value makes it possible to determine hydrate formation efficiency (E):

$$\begin{cases} \dfrac{K'_S}{K_S} \le 1 \Rightarrow E = \dfrac{K'_S}{K_S} \\ \dfrac{K'_S}{K_S} > 1 \Rightarrow E = \dfrac{K_S}{K'_S} \end{cases} \tag{16}$$

The use of calculated dependences for experimental data for GM synthesis in the diffusion mode (Fig. 8) demonstrates that the optimal supercooling is temperature difference of 2.9–3.0 °C. At higher supercooling values, the optimal ratio of heat removal and mass exchange is broken, with increase in time, the gas flow into GM slows down as a result of GM crust formation.

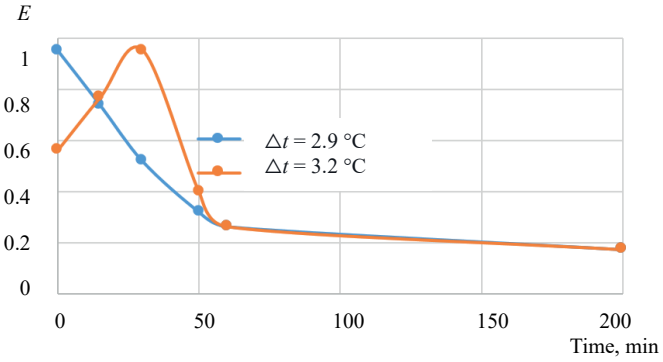
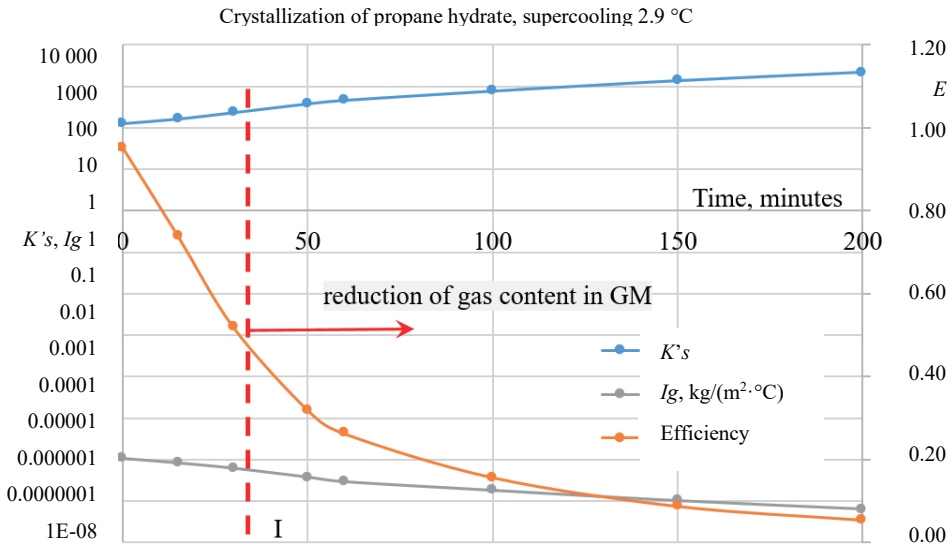


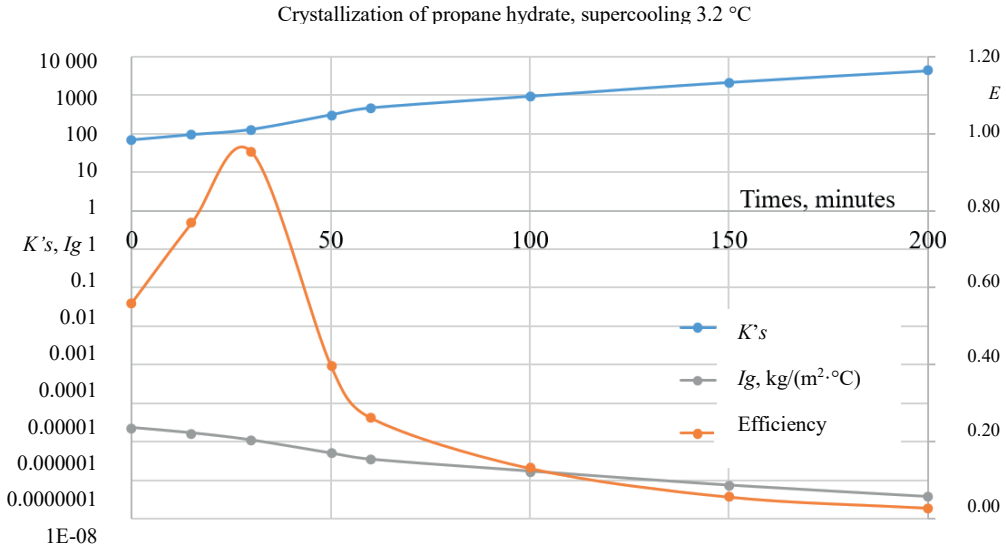
Fig. 8. The efficiency of the hydrate formation process in diffusion mode (E) depending on gas supercooling (Δt) and time according to experimental study results.

Fig. 9 shows graphs of GM synthesis process intensity by the value of optimization coefficient K'_S. As it is shown in the graph, the movement of values of graph functions to the right of the optimal zone I corresponds to a decrease in the rate of GM synthesis and gas content in the gas hydrate structure.

As it is shown in graph Fig. 9(b), non-observance of optimal K'_S values can also be at the initial moment of time, when the phase interface surface is 'clean', in this case the hydrate crust grows slowly and has little effect on the synthesis process intensity.



(a)



(b)

Fig. 9. Optimal characteristics of GH synthesis process at various levels of gas subcooling: (a) – 2.9 °C; (b) – 3.2 °C.

Thus, compliance with optimal K'_S values and renewal of the interface ensure the best intensity of hydrate formation. According to our technology (Fig. 1), additional gas cooling (if necessary) is performed in thermostat 8 and thus K'_S value can be adjusted. This criterion for optimization of heat and mass transfer processes in GM synthesis on the interfacial surface allows to determine the process parameters, complying with the above requirements to increase the intensity of the hydrate formation process. The proposed criterion can be applied to the GM bubbler design.

5. CONCLUSION

Diffusion phenomena underlying the processes of gas hydrate formation at the interface are slow and practically all researchers use various tools to intensify these processes. In most cases, these techniques make it possible to implement a diffusion-convective mechanism for heat and mass transfer between gas and liquid. Clearly, the intensity of these processes is affected by the temperatures of contacting phases and pressure in the reaction zone. However, with the diffusion-convective mechanism of gas hydrate formation, as well as with the diffusion mechanism, the synthesis intensity decreases as a hydrate layer at the interface, generating resistance to mass gas flow and prevents intense heat removal from the reaction zone. Therefore, the formed hydrate layer shall be destroyed and, thus, the phase interfacial contact will be renewed. According to our technology, this problem is solved using the hydrodynamic initiation of the synthesis process, resulting in a hydrodynamic and thermodynamic situation in the reactor, it contributes to deformation of gas droplets and breaking of hydrate films. Hydrate removal from the phase interface also means a rather intensive heat removal from the reaction zone.

It was determined that at a certain optimal ratio of the intensity values of heat and mass transfer processes at the phase contact interface, the synthesis rate will be maximum, continuous renewal of the contact interface allows maintaining the maximum value of this parameter throughout the entire synthesis process. In this case, the optimal values of gas subcooling are recorded at 2.5–3.5 °C. To assess the conditions for intensive GM synthesis, an optimization criterion is proposed to characterize the ratio of mass and heat transfer processes at the interface. Thus, this surface renewal and compliance with optimal ratios of heat and mass transfer processes, will make it possible to achieve the maximum rate of hydrate synthesis, these ratios can be adjusted using our proposed method.

ACKNOWLEDGEMENT

This research was funded by grant number 025/RID/2018/19 “Regional Initiative of Excellence” in 2019–2022.

REFERENCES

[1] Koh C. A., Sum A. K., Sloan E. D. State of the art: Natural gas hydrates as a natural resource. *J. Nat. Gas Sci. Eng*. 2012:8:132–138. https://doi.org/10.1016/j.jngse.2012.01.005

[2] Boswell R., *et al*. 6 - Natural Gas Hydrates: Status of Potential as an Energy Resource. *Future Energy* (Third Edition) Improved. Sustainable and Clean Options for our Planet. Elsevier, 2020:111–131. https://doi.org/10.1016/B978-0-08-102886-5.00006-2

[3] Xu H., *et al.* Decomposition characteristics of natural gas hydrates in hydraulic lifting pipelines. *Natural Gas Industry B* 2019:6(2):159–167. https://doi.org/10.1016/j.ngib.2018.07.005

[4] Pavlenko A., Koshlak H. Application of Thermal and Cavitation Effects for Heat and Mass Transfer Process Intensification in Multicomponent Liquid Media. *Energies* 2021:14(23):7996. https://doi.org/10.3390/en14237996.

[5] Boswell R., Collett T. S. Current perspectives on gas hydrate resources. *Energy Environ. Sci*. 2011:4:1045–1528. https://doi.org/10.1039/C0EE00203H

[6] Zhao J., *et al.* Analysing the process of gas production for natural gas hydrate using depressurization. *Appl. Energy* 2015:142:125–134. https://doi.org/10.1016/j.apenergy.2014.12.071

[7] Pavlenko A. Self-preservation Effect of Gas Hydrates. *Rocznik Ochrona Środowiska* 2021:23:346–355. https://doi.org/10.54740/ros.2021.023

[8] Chong Z. R., *et al.* Review of natural gas hydrates as an energy resource: Prospects and challenges. *Appl. Energy* 2016:162:1633–1652. https://doi.org/10.1016/j.apenergy.2014.12.061

[9] Chong Z. R., *et al.* Review of natural gas hydrates as an energy resource: Prospects and challenges. *Applied Energy* 2016:162:1633–1652. https://doi.org/10.1016/j.apenergy.2014.12.061

[10] Siažik J., Malcho M. Accumulation of primary energy into natural gas hydrates. *Procedia Engineering* 2017:192:782–787. https://doi.org/10.1016/j.proeng.2017.06.135

[11] Zhou S., *et al.* Research on the solid fluidization well testing and production for shallow non-diagenetic natural gas hydrate in deep water area China Offshore. *Oil Gas* 2017:29:(4):1–8.
[12] Bahadori A. Chapter 13—Liquefied Natural Gas (LNG). In *Natural Gas Processing Technology and Engineering Design*, 2014:591–632. https://doi.org/10.1016/B978-0-08-099971-5.00013-1
[13] Kiran B. S., *et al.* Experimental investigations on tetrahydrofuran-methane-water system: Rapid methane gas storage in hydrates. *Oil Gas Sci. Technol.-Rev. IFP Energ. Nouv*. 2019:74:12. https://doi.org/10.2516/ogst/2018092
[14] Zhang P., *et al.* Heat transfer and water migration rules during formation/dissociation of methane hydrate under temperature fields with gradient. *International Journal of Heat and Mass Transfer* 2021:169:120929. https://doi.org/10.1016/j.ijheatmasstransfer.2021.120929
[15] Zhao J., *et al.* In-situ visual observation for the formation and dissociation of methane hydrates in porous media by magnetic resonance imaging. *Magn. Reson. Imaging* 2015:33(4):485–490. https://doi.org/10.1016/j.mri.2014.12.010
[16] Rossi F., Filipponi M., Castellani B. Investigation on a novel reactor for gas hydrate production. *Applied Energy* 2012:99:167–172. https://doi.org/10.1016/j.apenergy.2012.05.005
[17] Koh D. Y., *et al.* Energy–efficient natural gas hydrate production using gas exchange. *Applied Energy* 2016:162:114–130. https://doi.org/10.1016/j.apenergy.2015.10.082
[18] Kumar K. V., *et al.* Nanoporous materials for the onboard storage of natural gas. *Chem. Rev*. 2017:117:1796–1825. https://doi.org/10.1021/acs.chemrev.6b00505
[19] Song Y. M., *et al.* Energy-efficient storage of methane in the formed hydrates with metal nanoparticles-grafted carbon nan- otubes as promoter. *Applied Energy* 2018:224:175–183. https://doi.org/10.1016/j.apenergy.2018.04.068
[20] Chong Z. R., *et al.* Review of natural gas hydrates as an energy resource: prospects and challenges. *Applied Energy* 2016:162:1633–1652. https://doi.org/10.1016/j.apenergy.2014.12.061
[21] Baek S., *et al.* Enhanced methane hydrate formation with cyclopentane hydrate seeds. *Applied Energy* 2017:202:32–41. https://doi.org/10.1016/j.apenergy.2017.05.108
[22] Veluswamy H. P., *et al.* An innovative approach to enhance methane hydrate formation kinetics with leucine for energy storage application. *Applied Energy* 2017:188:190–199. https://doi.org/10.1016/j.apenergy.2016.12.002
[23] Veluswamy H. P., *et al.* A review of solidified natural gas (SNG) technology for gas storage via clathrate hydrates. *Applied Energy* 2018:216:262–285. https://doi.org/10.1016/j.apenergy.2018.02.059
[24] Kiran B. S., *et al.* Experimental investigations on tetrahydrofuran – methane – water system: Rapid methane gas storage in hydrates. *Oil Gas Sci. Technol. – Rev. IFP Energies nouvelles* 2019:74:12. https://doi.org/10.2516/ogst/2018092
[25] He Y., *et al.* Surfactan- t-based promotion to gas hydrate formation for energy storage. *J. Mater. Chem*. 2019:A7:21634–21661. https://doi.org/10.1039/C9TA07071K
[26] Zhang J. S., Lee S., Lee J. W. Kinetics of methane hydrate formation from SDS solution. *Ind. Eng. Chem. Res*. 2007:46:6353–6359. https://doi.org/10.1021/ie070627r
[27] Jin Y., Konno Y., Nagao J. Growth of methane clathrate hydrates in porous media. *Energ. Fuel*. 2012:26:2242–2247. https://doi.org/10.1021/ef3001357
[28] Arora A., *et al.* Biosurfactant as a promoter of methane hydrate formation: thermodynamic and kinetic studies. *Sci Rep* 2016:6:20893. https://doi.org/10.1038/srep20893
[29] Kumar A., *et al.* Role of surfactants in promoting gas hydrate formation. *Ind. Eng. Chem. Res.* 2015:54:12217–12232. https://doi.org/10.1021/acs.iecr.5b03476
[30] Veluswamy H. P., Hong Q. W., Linga P. Morphology study of methane hydrate formation and dissociation in the presence of amino acid. *Cryst Growth Des* 2016:16:5932–5945. https://doi.org/10.1021/acs.cgd.6b00997
[31] Liu Y., *et al.* Methane storage in a hydrated form as promoted by leucines for possible application to natural gas transportation and storage. *Energy Technol.* 2015:3(8):815–819. https://doi.org/10.1002/ente.201500048
[32] Veluswamy H. P., *et al.* Effect of biofriendly amino acids on the kinetics of methane hydrate formation and dissociation. *Ind Eng Chem Res* 2017:56(21):6145–6154. https://doi.org/10.1021/acs.iecr.7b00427
[33] Mohammad-Taheri M., *et al.* Methane hydrate stability in the presence of water-soluble hydroxyalkyl cellulose. *J Nat Gas Chem* 2012:21(2):119–125. https://doi.org/10.1016/S1003-9953(11)60343-5
[34] Sharma D., *et al.* Methane storage in mixed hydrates with tetrahydrofuran. *Indian J Chem Technol* 2014:21:114–119.
[35] Sowjanya Y., Prasad P. S. R. Formation kinetics & phase stability of double hydrates of C4H8O and CO2/CH4: A comparison with pure systems. *Journal of Natural Gas Science and Engineering* 2014:18:58–63. https://doi.org/10.1016/j.jngse.2014.02.001
[36] Veluswamy H. P., *et al.* Enhanced clathrate hydrate formation kinetics at near ambient temperatures and moderate pressures: Application to natural gas storage. *Fuel* 2016:182:907–919. https://doi.org/10.1016/j.fuel.2016.05.068
[37] Delahaye A., *et al.* Effect of THF on equilibrium pressure and dissociation enthalpy of CO_2 hydrates applied to secondary refrigeration. *Ind. Eng. Chem. Res*. 2006:45:391–397. https://doi.org/10.1021/ie050356p
[38] Sharma D., *et al.* Methane storage in mixed hydrates with tetrahydrofuran. *Indian J. Chem. Technol*. 2014:21:114–119.
Kiran B. S., *et al.* Experimental investigations on tetrahydrofuran – methane – water system: Rapid methane gas storage in hydrates. *Oil Gas Sci. Technol. – Rev. IFP Energies nouvelles* 2019:74:12. https://doi.org/10.2516/ogst/2018092
[39] Lucia B., *et al.* Experimental investigations on scaled-up methane hydrate production with surfactant promotion: Energy considerations. *Journal of Petroleum Science and Engineering* 2014:120:187–193. https://doi.org/10.1016/j.petrol.2014.06.015

[40] Rossi F., Filipponi M., Castellani B. Investigation on a novel reactor for gas hydrate production. *Applied Energy* 2012:99:167–172. https://doi.org/10.1016/j.apenergy.2012.05.005

[41] Luo Y. T., *et al.* Study on the kinetics of hydrate formation in a bubble column. *Chemical Engineering Science* 2007:62(4):1000–1009. https://doi.org/10.1016/j.ces.2006.11.004

[42] Cheng C., *et al.* Review and prospects of hydrate cold storage technology. *Renewable and Sustainable Energy Reviews* 2020:117:109492. https://doi.org/10.1016/j.rser.2019.109492

[43] Pavlenko A., Koshlak H. Intensification of Gas Hydrate Formation Processes by Renewal of Interfacial Area between Phases. *Energies* 2021:14(18):5912. https://doi.org/10.3390/en14185912

[44] Murakami T., *et al.* Forming a Structure-H Hydrate Using Water and Methylcyclohexane Jets Impinging on Each Other in a Methane Atmosphere. *Energy & Fuels* 2009:23:1619–1625. https://doi.org/10.1021/ef800880f

[45] Pavlenko A. Thermodynamic Features of the Intensive Formation of Hydrocarbon Hydrates. *Energies* 2020:13:3396. https://doi.org/10.3390/en13133396